Dalton Transactions

Accepted Manuscript

ROYAL SOCIETY OF CHEMISTRY

www.rsc.org/dalton

Journal Name

RSCPublishing

COMMUNICATION

Calix[2]triazole[2]arene-Based Fluorescent Chemosensor for Probing the Copper Trafficking Pathway in Wilson's Disease†

Cite this: DOI: 10.1039/x0xx00000x

Received 00th January 2012,
Accepted 00th January 2012

DOI: 10.1039/x0xx00000x

www.rsc.org/

Jihee Cho[‡,a] Tuhin Pradhan,[‡,b] Yun Mi Lee,[a] Jong Seung Kim,*[,b] and Sanghee Kim*[,a]

A pyrenyl-appended calix[2]triazole[2]arene displaying excellent selectivity for Cu^{2+} over other metal ions in pyrenyl excimer emission changes was synthesized. The binding mode with Cu^{2+} was supported through nuclear magnetic resonance (NMR) studies and density functional theory (DFT) calculations. Fluorescence imaging demonstrates that this new copper sensor is capable of detecting intracellular copper in living cells. Furthermore, through colocalization of the probe with organelle trackers as a function of time, it was observed that copper initially accumulates in lysosomes and then decreases. These results provide evidence for a close relationship between copper and lysosomes in Wilson's disease. This system is the first Cu^{2+} ion-induced fluorescent turn-on system used for imaging copper trafficking over time in a Wilson's disease model.

Copper is a vital element required for various cellular events.[1] Failure to maintain appropriate copper levels is associated with many diseases such as Alzheimer's[2] and Wilson's disease.[3] The latter is a disorder of copper metabolism caused by mutations in the ATP7B gene. It was proposed that when the intracellular level of copper reaches a certain threshold, copper uptake stops and intracellular copper accumulates in lysosomes.[4] As a result of the accumulation of redox-active copper in lysosomes, lipids in lysosomal membrane are peroxidated, causing lysosomal rupture and apoptosis.[5,6] Although several reports have elucidated the mechanism of cellular copper transport and metabolism in Wilson's disease,[5b,7] many aspects still remain understudied.

Calixarenes have long been employed as templates in the development of molecular sensors.[8] We recently prepared calix[2]triazole[2]arene (**1**, Scheme 1), a new hybrid calixarene, and demonstrated its unique properties compared to conventional calixarenes.[9,10] 1,2,3-Triazole-containing compounds have been reported to exhibit a high affinity for metal ions. Some triazole derivatives display Cu^{2+} selectivity over other metal ions.[11,12] Due to their selectivity toward Cu^{2+} binding, in this study, triazole rings were utilized as part of the main framework of the calixarene scaffold as a copper sensing moiety. For signaling, we introduced two pendant pyrenes to the lower rim of the hybrid calixarene to give the pyrenyl-appended calix[2]triazole[2]arene **2**. We hypothesized that the interaction of triazole rings with metal ions could promote a conformational annulus change of **2** to give fluorescence changes upon pyrenyl excimer emission. Herein, we report a new fluorescent Cu^{2+} ion sensor, **2**, that may be useful for generating evidence supporting a pathway of copper trafficking in a Wilson's disease model. As far as we know, this system is the first Cu^{2+} ion-induced fluorescent turn-on system for imaging copper trafficking over time in a model of Wilson's disease.[13]

The chemosensor **2** was prepared in a quantitative yield by reaction of **1** with bromomethylpyrene **3**[14] (Scheme 1). Under these reaction conditions, we did not detect the formation of other conformational isomers that have pyrenylmethyl groups on opposite sides of the annulus.

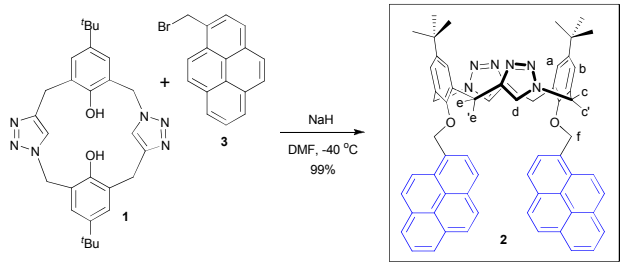

Scheme 1 Synthesis of pyrenyl-appended calix[2]triazole[2]arene **2**.

The ^{1}H NMR spectrum of **2** at room temperature suggests a C_2 symmetry in the molecule (Fig. S20). A NOESY experiment revealed that **2** is in a conformation that positions the phenolic oxygen atoms and triazole protons on the same side of the annulus as depicted in Scheme 1 (see also Fig. S24). As shown in Fig. 1, the fluorescence spectrum of **2** exhibits weak monomer emission at 377 and 396 nm and strong emission at 476 nm. These characteristics are typical of pyrene excimer emission from the intramolecular π-stacking of two pyrene units.[15,16]

The metal ion binding properties of **2** were examined using perchlorate salts of various metal cations (100 equiv.) in acetonitrile solution. Most metal ions tested with **2** did not show significant fluorescence changes (Fig. 1 and S2). However, Cu^{2+} showed a blue shift of pyrenyl excimer emission from 476 to 450 nm. Notably, **2** distinguished Cu^{2+} from Cu^{+} with respect to the excimeric emission changes, which has rarely been reported in the literature.[17]

The formation of a dynamic or a static excimer of pyrenes is dependent on the distance between the two pyrenes upon complexation of guest ions. The fluorescence maximum at 450 nm in this study is characteristic of a static pyrene excimer.[18,19] Evidence for the shift from dynamic to static excimer upon the addition of Cu^{2+} ions was induced from the following experiment. Time-resolved fluorescence decay measurements were performed with **2** in acetonitrile to monitor the lifetime change of **2** upon stepwise addition of Cu^{2+}. We collected emission decays of **2** in the presence of Cu^{2+} at 450 nm (excimer emission peak) using 375 nm laser light as the excitation source. The longer time constants (~25 ns, Table S1) of the bi-exponential decay fit are associated with the lifetime of the pyrenyl excimer,[20] and the shorter time constant (~3 ns) is related to the rate of excimer-monomer formation. However, we observed little change in the lifetime (longer time constant) of **2** upon the addition of highly concentrated Cu^{2+} solutions (up to 1.5 mM) (Table S1). This observation strongly supports the static excimer formation of **2** in the presence of Cu^{2+} ions.[18]

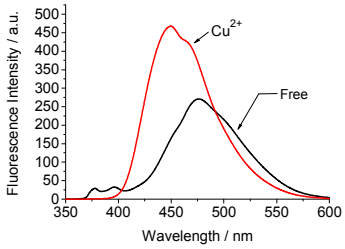

Fig. 1 Fluorescence spectra of **2** (6.0 μM) in acetonitrile and in the presence of 100 equiv of Cu^{2+} (excitation at 344 nm).

The fluorescence intensity maximum for the static excimer was reached in the presence of approximately 120 equivalents of Cu^{2+} ions (Fig. S3b). Using the fluorescence titration data (Fig. S3b), the binding constant (K_a)[21] in acetonitrile was calculated to be 3.71×10^4 M^{-1} (Fig. S4). The stoichiometry between probe **2** and Cu^{2+} was indicated by Job's plot experiment and MALDI-TOF mass spectroscopy. Job's plot experiment showed a maximum at 0.5 mole fraction of Cu^{2+}, indicating a 1:1 stoichiometric ratio between probe **2** and Cu^{2+} in acetonitrile solution (Fig. S8). MALDI-TOF mass showed a peak at m/z 975.4432 corresponding to [probe **2**+Cu^{2+}-2H]$^+$ which gave further evidence of the formation of 1:1 complex between **2** and Cu^{2+} (Fig. S11). Competition experiments for Cu^{2+} ions with other common metal ions showed no significant variation in the static excimer emission of **2** (Fig. S6).[22] The binding mode of **2** to Cu^{2+} ions was deduced from NMR studies (Fig. S19). In the presence of excess Cu^{2+}, the binding mode could not be determined due to the paramagnetic nature of Cu^{2+}. Fortunately, some informative changes were obtained upon the addition of small quantities of Cu^{2+}. In the presence of 0.06 equivalents of Cu^{2+}, the signal from the triazole hydrogen atoms (H_d) of **2** shifted downward (0.13 ppm) with peak broadening. These spectral changes led us to propose that the Cu^{2+} is bound to nitrogen atoms in the calixtriazoles.

To gain further insight into the origin of static pyrenyl excimer formation upon the addition of Cu^{2+} ions to **2**, density functional theory (DFT)-based theoretical calculations were performed. The optimized structures of **2** and the **2**-Cu^{2+} complex are shown in Fig. 2. In the proposed binding mode, two oxygen atoms in the peripheral calixarene ring and one triazole ring in the annulus are involved in Cu^{2+} binding. Three theoretical parameters,[10] dihedral angle (DHA), vertical displacement (Δ; Å), and minimum distance (D), were used to check the possibility of intramolecular excimer formation between the two pyrenes of **2** and the **2**-Cu^{2+} complex. DHA (angles denoted by blue dotted lines connecting the C_1, C_2, C_3 and C_4 carbons, as shown in Fig. 2) can be related with parallelism of two pyrenes. The DHA values for **2** and the **2**-Cu^{2+} complex are 43.6° and 32.0°, respectively, revealing that the two pyrene moieties are more parallel in the **2**-Cu^{2+} complex than in **2**. The zero vertical displacement ensures the maximum overlap integral interval between two parallel pyrenes. The vertical displacements for **2** and the **2**-Cu^{2+} complex are nearly identical (~1.4 Å). The minimum distance (D) is the closest distance between the two pyrenes (Fig. 2). The minimum distances calculated for **2** and the **2**-Cu^{2+} systems are in the range of excimer formation,[18] but the distance in the **2**-Cu^{2+} complex is shorter than that in **2**, implying that the **2**-Cu^{2+} complex facilitates better excimer formation than **2**. The calculated binding energy (–364.33 kcal mol^{-1} in the gas phase) supports the strong binding of Cu^{2+} with **2**. For verification studies, we eliminated Cu^{2+} from the **2**-Cu^{2+} system and repeated the optimization of the metal-free system without perturbing any additional geometrical parameters. We observed that eliminating metal ions induces significant changes in the theoretical parameters (DHA increases from 32.0° to 52.9°, and the minimum distance increases from 3.98 to 4.80 Å). This result indicates that the strong binding of Cu^{2+} with **2** is a possible driving force for achieving shorter distances and more parallelism between two pyrenes compared to **2**. Subsequently, this binding led to better excimer formation in the **2**-Cu^{2+} complex.

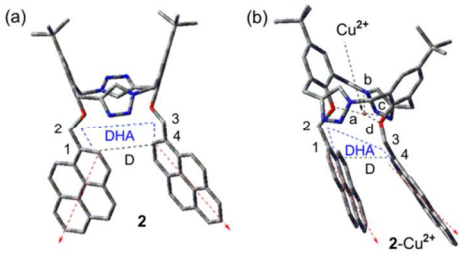

Fig. 2 Optimized structures of (a) **2** and (b) the Cu^{2+} complex with **2**. Structures were optimized at the B3LYP/6-31G(d) level of theory. Gray, red, and blue represent carbon, oxygen and nitrogen atoms, respectively. Hydrogen atoms were removed from the diagram for clarity. Black dotted lines indicate the bond distances (a, b, c and d) between Cu^{2+} and **2**. Bond distances (a, b, c and d) in (b) are 2.03, 2.74, 2.78 and 2.04 Å, respectively. Red arrows indicate the directions of the planes containing pyrenes. Blue dotted lines indicate the dihedral angles (DHA) among the carbons numbered 1, 2, 3 and 4. The bold black dotted line indicates the minimum distance (D) between two pyrenes.

The selectivity of **2** for Cu^{2+} over other metal ions and its emission changes led us to examine the possibility of employing **2** as a copper-ion sensor in living cells. Initially, the cytotoxicity of **2** was determined by a sulforhodamine B (SRB) assay. Probe **2** at concentrations less than 20 μM did not exhibit distinct cytotoxicity (Fig. S18). Based on this result, the cellular behaviors of **2** towards HepG2, such as cellular acceptance and distribution, were tested with a 10 μM solution of **2**. We found that probe **2** was readily incorporated into cells and provided a stable read-out system by which to image cellular distribution. Clear fluorescence images at 525±10 nm were observed after 1.5 h incubation. The image showed broad cytoplasmic distribution of **2** (Fig. S14).

After discerning the basic properties of **2** in cell imaging, we investigated the behavior of **2** with copper in cultured cells. While weak intracellular fluorescence at 434±9 nm was observed when HepG2 cells were incubated with **2**, strong fluorescence was detected upon the addition of **2** to the $CuCl_2$ (200 μM)-pre-treated HepG2 cells (Fig. 3a *vs.* 3b). The fluorescence intensity was observed to decrease when the metal-chelating agent ethylenediaminetetraacetic acid (EDTA) (1.0 mM) was added to the

fluorescent cells (Fig. 3c), demonstrating that probe **2** can be used to image intracellular copper in living cells.

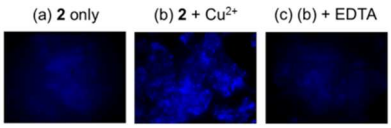

Fig. 3 Fluorescence images of copper in HepG2 cells. (a) HepG2 cells incubated with **2** (10 μM) for 1.5 h at 37 °C. (b) HepG2 cells incubated with $CuCl_2$ (200 μM) for 1 h and then further incubated with **2** (10 μM) for 1.5 h at 37 °C. (c) **2** (10 μM) + $CuCl_2$ (200 μM) pre-treated HepG2 cells incubated with EDTA (1.0 mM) for 0.5 h at 37 °C. Fluorescence emission was detected in the blue region (λ_{ex}=340±13 nm, λ_{em}=434±9 nm).

Treatment of 200 μM copper produces copper concentrations in HepG2 cells that are approximately six times higher than normal copper levels, which is a similar result to that observed in Wilson's disease.[23] Thus, the $CuCl_2$-pre-treated HepG2 cells could be considered a cellular model of Wilson's disease. With these copper-enriched cells and the copper-selective probe **2**, we attempted to track the pathogenic behavior of copper. According to results from propidium iodide (PI) staining experiments (Fig. S17), the optimal copper concentration was 200 μM. The time frame of the copper colocalization study was set to be within 24 h, as after that period, obvious cell death was observed at 200 μM copper.

Previous groups have reported that the lysosome is the major site of copper accumulation.[4] Thus, the distribution of copper in lysosomes was monitored over time to better understand copper-mediated cell death in Wilson's disease. HepG2 cells were treated with $CuCl_2$ (200 μM) at various time periods (0 min–24 h), followed by incubation with probe **2** (10 μM) and Lyso Tracker Red DND-99, respectively. For quantitative colocalization analysis, Pearson's coefficients[24] were calculated using fluorescence images.[25] We observed that the Pearson's coefficient value (r) of lysosomes rapidly increased in the initial hour and then gradually decreased to a level similar to that at 10 min (Fig. 4).[26] These results imply that copper initially accumulated in lysosomes and then slowly disappeared. This disappearance could have several origins.[27] One potential reason underlying the disappearance of Cu^{2+} is the oxidative damage to lysosomal membrane lipids by the accumulated redox-active copper, which could be followed by diffusion of copper to the surroundings through the damaged membrane. The copper-induced lysosomal membrane damage has been described in previous studies.[5] These studies reported that lysosomal Cu^{2+} reacts with H_2O_2 to produce toxic reactive oxygen species (ROS), and the ROS damages the lysosomal membrane. Although our current data did not clearly present a pathway for copper-mediated apoptosis, they may at least support previous biochemical studies that suggested a close relationship between copper and lysosomes in Wilson's disease.

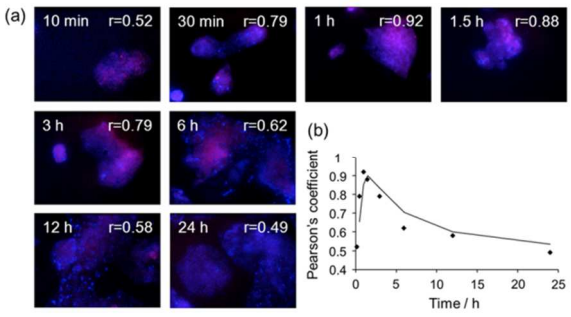

Fig. 4 The release of lysosomal copper into the surroundings after copper-induced apoptosis. (a) Localization studies of **2** in copper-induced apoptotic HepG2 cells. HepG2 cells incubated with $CuCl_2$ (200 μM) for different time periods (0 min–24 h) and with **2** (10 μM) for 1.5 h and then further incubated with Lyso Tracker Red DND-99 (0.1 μM) for 0.5 h at 37 °C. These pictures are merged images between the blue emission of **2** + Cu^{2+} (λ_{ex}=340±13 nm, λ_{em}=434 ±9 nm) and the red emission of Lyso Tracker (λ_{ex}=543±22 nm, λ_{em}=593±40 nm). The violet regions represent the colocalization of **2** with Lyso Tracker. The degree of overlap of blue and red signal is presented as the Pearson's correlation coefficient (r). (b) A plot of Pearson's correlation coefficients for the estimation of the colocalization of **2** with Lyso Tracker.

In conclusion, although several biological studies have been undertaken on Wilson's disease over the last several decades, there are still unanswered questions about the detailed functions and mechanisms of copper in hepatocytes. This gap is partly due to the scarcity of probes, which allow imaging of the distribution and level of copper in cells. To address this gap, we synthesized the fluorescent chemosensor **2**, which displays high selectivity for Cu^{2+} over other metal ions and was capable of imaging intracellular copper in living cells. Through colocalization experiments of probe **2** with organelle trackers, we were able to quantify the copper level in the lysosomes of hepatocytes at a variety of time periods. This colocalization study as a function of time indicated that the lysosomal copper level initially rapidly increased and then declined during a follow-up period, demonstrating the accumulation and disappearance of copper over the specified time period in lysosomes. The accumulation of redox-active copper causes oxidative damage to the lysosomal membrane lipids, and the copper diffuses into the surroundings through the damaged membrane. Although additional studies are necessary to clearly elucidate the pathway of copper trafficking in Wilson's disease, our preliminary results could provide a basis for the further investigation of Wilson's disease as well as other copper-related disorders. Additionally, based upon these preliminary results, probe **2** will be a useful chemical tool for studying the roles of copper in biological systems.

This research was supported by a National Research Foundation of Korea (NRF) grant funded by the Korea government (MSIP) (No. 2007-0056817) and the CRI Program (No. 2009-0081566).

Notes and references

[a] College of Pharmacy, Seoul National University, Seoul 151-742, Korea. E-mail: pennkim@snu.ac.kr
[b] Department of Chemistry, Korea University, Seoul 136-701, Korea. E-mail: jongskim@korea.ac.kr

† Electronic Supplementary Information (ESI) available: Experimental procedure, characterization data, computational details, fluorescence images and additional spectra (UV/vis absorption, fluorescence, NMR). See DOI: 10.1039/c000000x/

‡ These authors contributed equally.

1 (a) *Biological inorganic chemistry: structure and reactivity*, ed. H. B. Gray, E. I. Stiefel, J. S. Valentine and I. Bertini, University science books, Mill Valley, 2007; (b) *The biological chemistry of the elements*, ed. J. J. R. F. da Silva and R. J. P. Williams, Oxford, Clarendon, 1991; (c) M. L. Turski and D. J. Thiele, *J. Biol. Chem.,* 2009, **284**, 717; (d) E. L. Que, D. W. Domaille and C. J. Chang, *Chem. Rev.,* 2008, **108**, 1517; (e) A. V. Davis and T. V. O'Halloran, *Nat. Chem. Biol.,* 2008, **4**, 148.
2 (a) L. M. Klevay, *Med. Hypotheses,* 2008, **70**, 802; (b) E. Gaggelli, H. Kozlowski, D. Valensin and G. Valensin, *Chem. Rev.,* 2006, **106**, 1995.
3 (a) T. Hirayama, G. C. Van de Bittner, L. W. Gray, S. Lutsenko and C. J. Chang, *Proc. Natl. Acad. Sci. U. S. A.,* 2012, **109**, 2228; (b) G. Crisponi, V. M. Nurchi, D. Fanni, C. Gerosa, S. Nemolato and G. Faa, *Coord. Chem. Rev.,* 2010, **254**, 876; (c) A. Ala, A. P. Walker, K. Ashkan, J. S. Dooley and M. L. Schilsky, *Lancet,* 2007, **369**, 397.

4 (a) M. Ralle, D. Huster, S. Vogt, W. Schirrmeister, J. L. Burkhead, T. R. Capps, L. Gray, B. Lai, E. Maryon and S. Lutsenko, *J. Biol. Chem.,* 2010, **285**, 30875; (b) M. Yano, N. Sakamoto, T. Takikawa and H. Hayashi, *Nagoya J. Med. Sci.,* 1993, **55**, 131; (c) A. Yagi, H. Hayashi, T. Higuchi, N. Hishida and N. Sakamoto, *Int. J. Exp. Path.,* 1992, **73**, 85; (d) J. S. Kumaratilake and J. M. Howell, *J. Comp. Path.,* 1989, **100**, 381; (e) S. Goldfischer and I. Sternlieb, *Am. J. Pathol.,* 1968, **53**, 883.
5 (a) D. C. Kennedy, R. K. Lyn and J. P. Pezacki, *J. Am. Chem. Soc.,* 2009, **131**, 2444; (b) D. Huster and S. Lutsenko, *Mol. BioSyst.,* 2007, **3**, 816; (c) W. Y. Boadi, S. Harris, J. B. Anderson and S. E. Adunyah, *Drug Chem. Toxicol.,* 2013, **36**, 155; (d) R. Hong, T. Y. Kang, C. A. Michels and N. Gadura, *Appl. Environ. Microbiol.,* 2012, **78**, 1776; (e) H. Zhang, Y. Xia, G. Wang and Z. Shen, *Planta,* 2008, **227**, 465; (f) R. Seth, S. Yang, S. Choi, M. Sabean and E. A. Roberts, *Toxicol. Vitro,* 2004, **18**, 501; (g) J. Pourahmad, S. Ross and P. J. O'Brien, *Free Radic. Biol. Med.,* 2001, **30**, 89; (h) J. Pourahmad and P. J. O'Brien, *Toxicology,* 2000, **143**, 263; (i) D. Klein, J. Lichtmannegger, U. Heinzmann, J. Müller-Höcker, S. Michaelsen and K. H. Summer, *Eur. J. Clin. Invest.,* 1998, **28**, 302.
6 (a) U. Repnik and B. Turk, *Mitochondrion,* 2010, **10**, 662; (b) P. Boya and G. Kroemer, *Oncogene,* 2008, **27**, 6434; (c) M. E. Guicciardi, M. Leist and G. J. Gores, *Oncogene,* 2004, **23**, 2881.
7 (a) T. Y. Tao and J. D. Gitlin, *Hepatology,* 2003, **37**, 1241; (b) M. DiDonato and B. Sarkar, *Biochim. Biophys. Acta-Mol. Basis Dis.,* 1997, **1360**, 3.
8 For a comprehensive reviews on calixarenes, see: (a) *Calixarenes 2001*, ed. Z. Asfari, V. Bőhmer, J. Harrowfield and J. Vicens, Kluwer, Dordrecht, 2001; (b) *Calixarenes in Action*, ed. L. Mandolini and R. Ungaro, Imperial College Press, London, 2000; (c) *Calixarenes: An introduction (Monographs in Supramolecular Chemistry)*, ed. C. D. Gutsche, The Royal Society of Chemistry, Cambridge, 2nd edn, 2008.
9 J. Cho, S. Lee, S. Hwang, S. H. Kim, J. S. Kim and S. Kim, *Eur. J. Org. Chem.,* 2013, 4614.
10 J. Cho, T. Pradhan, J. S. Kim and S. Kim, *Org. Lett.,* 2013, **15**, 4058.
11 (a) R. K. Pathak, V. K. Hinge, P. Mondal and C. P. Rao, *Dalton Trans.,* 2012, **41**, 10652; (b) Y.-J. Zhang, X.-P. He, M. Hu, Z. Li, X.-X. Shi and G.-R. Chen, *Dyes Pigment.,* 2011, **88**, 391; (c) E. Hrishikesan, C. Saravanan and P. Kannan, *Ind. Eng. Chem. Res.,* 2011, **50**, 8225; (d) Y. H. Lau, J. R. Price, M. H. Todd and P. J. Rutledge, *Chem. Eur. J.,* 2011, **17**, 2850.
12 (a) Y. H. Lau, P. J. Rutledge, M. Watkinson and M. H. Todd, *Chem. Soc. Rev.,* 2011, **40**, 2848; (b) J. J. Bryant and U. H. F. Bunz, *Chem. Asian J.,* 2013, **8**, 1354.
13 For a previously reported Cu^{2+}-induced fluorescent turn-off system for the imaging of lysosomal copper level changes, see: X. Wang, X. Ma, Z. Yang, Z. Zhang, J. Wen, Z. Geng and Z. Wang, *Chem. Commun.,* 2013, **49**, 11263.
14 E. Soto, J. C. MacDonald, C. G. F. Cooper and W. G. McGimpsey, *J. Am. Chem. Soc.,* 2003, **125**, 2838.
15 (a) C. J. Broan, *Chem. Commun.*, **1996**, 699; (b) H. J. Kim, M. H. Lee, L. Mutihac, J. Vicens and J. S. Kim, *Chem. Soc. Rev.,* 2012, **41**, 1173; (c) J. S. Kim and D. T. Quang, *Chem. Rev.,* 2007, **107**, 3780; (d) D. T. Quang and J. S. Kim, *Chem. Rev.,* 2010, **110**, 6280; (e) S. Y. Park, J. H. Yoon, C. S. Hong, R. Souane, J. S. Kim, S. E. Matthews and J. Vicens, *J. Org. Chem.,* 2008, **73**, 8212.
16 The corresponding pyrenyl-appended calix[4]arene was also prepared. Although its two pyrene units are on the same side of the annulus as those of **2**, the fluorescence spectra exhibited only monomer emission without showing pyrene excimer emission (Fig. S7 and S25).
17 (a) W.-L. Chang and P.-Y. Yang, *J. Lumines.,* 2013, **141**, 38; (b) L. Tang, J. Guo and Z. Huang, *Bull. Korean Chem. Soc.,* 2013, **34**, 1061; (c) P. Li, H. Zhou and B. Tang, *J. Photochem. Photobiol. A-Chem.,* 2012, **249**, 36.
18 F. M. Winnik, *Chem. Rev.*, **1993**, *93*, 587.
19 The shift from dynamic to static excimer upon the addition of Cu^{2+} was evident in the excitation spectra (Fig. S5).
20 (a) T. Pradhan, H. A. R. Gazi and R. Biswas, *J. Chem. Phys.,* 2009, **131**, 054507; (b) R. Biswas, N. Rohman, T. Pradhan and R. Buchner, *J. Phys. Chem. B,* 2008, **112**, 9379; (c) T. Pradhan, P. Ghoshal and R. Biswas, *J. Phys. Chem. A,* 2008, **112**, 915; (d) T. Pradhan and R. Biswas, *J. Phys. Chem. A,* 2007, **111**, 11524; (e) K. Dahl, R. Biswas, N. Ito and M. Maroncelli, *J. Phys. Chem. B,* 2005, **109**, 1563.
21 H. A. Benesi and J. H. Hildebrand, *J. Am. Chem. Soc.,* 1949, **71**, 2703.
22 Anion effect of probe **2** was investigated using tetrabutylammonium salts of various anions (Br^-, Cl^-, F^-, I^-, ClO_4^-, $H_2PO_4^-$, HSO_4^-, NO_3^-, OAc^-) in acetonitrile solution. None of the anions above tested with **2** showed fluorescence changes (Fig. S9). In competition experiments, when various anions were added to a solution of **2**-Cu^{2+} complex, no excimer emission shift was observed (Fig. S10).
23 V. S. Narayanan, C. A. Fitch and C. W. Levenson, *J. Nutr.,* 2001, **131**, 1427.
24 K. W. Dunn, M. M. Kamocka and J. H. McDonald, *Am. J. Physiol.-Cell Physiol.,* 2011, **300**, C723.
25 The Pearson's coefficient values (*r*) were calculated using software (AutoQuant X3).
26 Our subcellular copper localization studies with probe **2** showed that the coefficient value (*r*) of lysosomes was the highest compared to other organelles after incubation with $CuCl_2$ for 1 h (Fig. S15).
27 One possibility is the reduction of Cu^{2+} to Cu^+ with concomitant oxidation of intracellular constituents.

Calix[2]triazole[2]arene-Based Fluorescent Chemosensor for Probing the Copper Trafficking Pathway in Wilson's Disease

Jihee Cho, Tuhin Pradhan, Yun Mi Lee, Jong Seung Kim,* and Sanghee Kim*

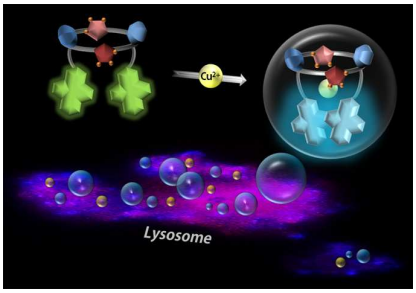

We herein present a synthesis of new fluorescent chemosensor for Cu^{2+} and its application to Wilson's disease cell model to probe the copper trafficking pathway.